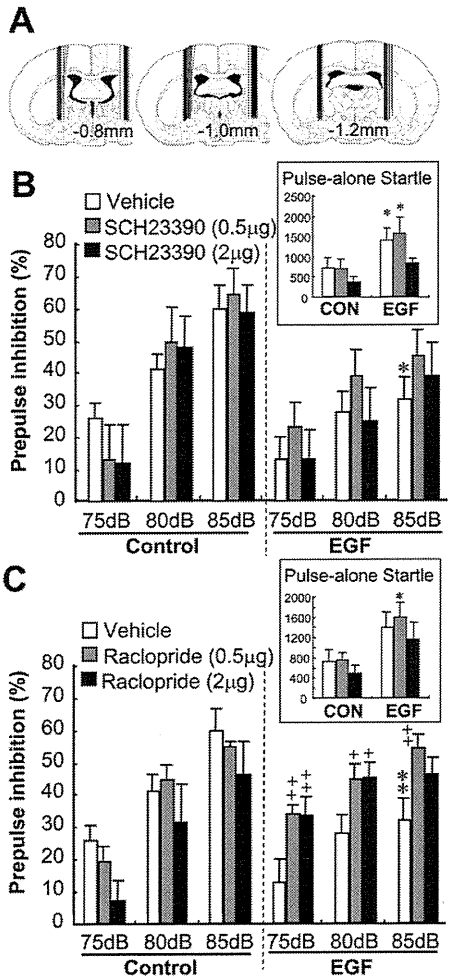

Figure 6. Effects of pallidal infusion of dopamine receptor antagonists on PPI deficits. Different doses of the D1-like receptor antagonist [SCH23390; 0 μg (vehicle), 0.5 μg or 2 μg per site] or the D2-like receptor antagonist [raclopride; 0 μg (vehicle alone), 0.5 μg or 2 μg per site] were administered to both hemispheres of the globus pallidus of EGF and control rats. (A) Cannula placement was confirmed in fixed brains, and four out of 69 rats were excluded from the final data analysis due to incorrect cannula placement. Rats receiving SCH23390 (B) or raclopride (C) were subjected to PPI test with 75-, 80- and 85-dB prepulse stimuli combined with a 120-dB startle tone. Pulse-alone startle responses to a 120-dB tone were measured in arbitrary units and are shown in the inset. Bars indicate mean ± SEM (N = 8–9 for each group). Data of rats receiving vehicle alone (control) were shared in (B) and (C). *P<0.05, **P<0.01, compared with vehicle-infused controls; +P<0.05, ++P<0.01, compared with vehicle-infused EGF rats by Fisher's LSD.
doi:10.1371/journal.pone.0025831.g006

argument that elevated dopamine release in the globus pallidus is responsible for the PPI deficits.

Difference in cataleptic actions of a D2-like receptor antagonist on EGF-treated and control rats

Because dopamine D2-like receptor blockade is known to induce cataleptic behaviors [36], we used the bar-hang immobility test to estimate the effects of the antagonist on catalepsy scores (Fig. 8A). Prior to drug administration, EGF-treated and control rats were

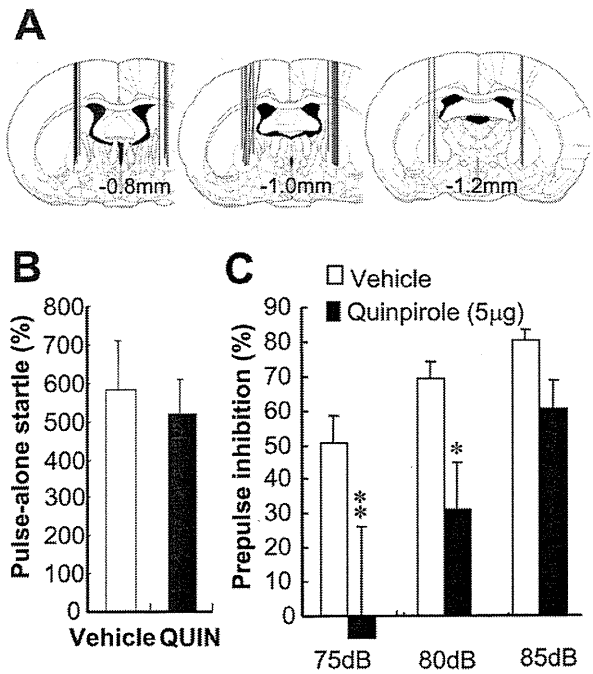

Figure 7. Effects of pallidal infusion of a dopamine D2-like agonist on PPI. A dopamine D2-like agonist, quinpirole (QUIN) (5 μg per site), or vehicle was administered to both hemispheres of the GP of naïve rats. (A) Cannula placement was confirmed in fixed brains, and one out of 18 rats was excluded from the final data analysis due to incorrect cannula placement. Fifteen minutes after quinpirole injection, pulse-alone startles (B) and PPI scores (C) were measured with 75-, 80- and 85-dB prepulse stimuli combined with a 120-dB startle tone. Bars indicate mean ± SEM (n = 8 or 9 each). *p<0.05, **p<0.01, compared with vehicle-infused controls by Fisher LSD.
doi:10.1371/journal.pone.0025831.g007

subjected to the first session of the bar-hang test. There was a significant basal difference in bar-hang latency [$F(1,43) = 19.0$, $P<0.001$ for EGF] (Fig. 8B). Pallidal infusion of the D2-like receptor antagonist produced differential effects on EGF and control rats [$F_{(2,44)} = 9.07$, $P<0.001$ for raclopride dose×EGF]. The higher dose of raclopride significantly increased bar-hang latency in control rats ($P<0.001$) but not in EGF rats. Thus, EGF rats appear to be insensitive to the given doses of the D2-like receptor blocker in this test. These results rule out the possibility that the observed raclopride effects on PPI in EGF-treated rats might reflect its cataleptic action. Moreover, this experiment revealed the lower sensitivity of EGF-treated rats to pallidal D2-like receptor blockade.

Of note, the pallidal infusion of the D2-like receptor agonist quinpirole to naïve rats significantly diminished the bar-hang latency, compared with the latency before injection [$F(2,24) = 4.54$, $P = 0.021$] (Fig. 8C). The bar-hang latency of quinpirole-infused rats was significantly shorter than that of vehicle-infused controls ($P<0.001$) and indistinguishable from that of EGF-treated rats. All these results suggest that pallidal dopaminergic signals negatively regulate bar-hang latency. Therefore, the shorter bar-hung latency of EGF-treated rats supports our argument that pallidal dopamine function was up-regulated in these animals.

Discussion

In the present investigation, we attempted to address the question of how EGF challenge at the perinatal stage alters later

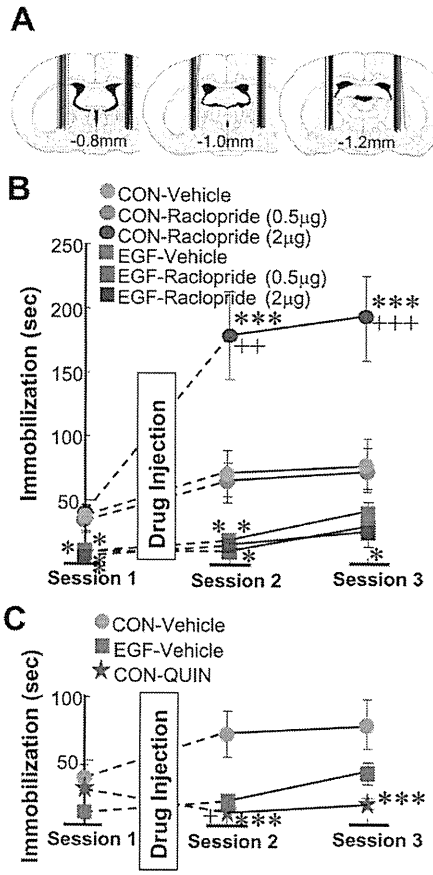

Figure 8. Measurement of immobility in the bar-hang test following pallidal infusion of the dopamine receptor antagonist and agonist. (A) Cannula placement was confirmed in fixed brains, and four out of 63 rats were excluded from the final data analysis due to incorrect cannula placement. The bar-hang test consisted of 3 blocks with 20-min intervals. Vehicle, raclopride (B; 0.5 and 2.0 μg per site) or quinpirole (QUIN) (C; 10.0 μg per site) was bilaterally injected into the globus pallidus of EGF and control (CON) rats after block #1. In each session we measured the latency until one of the paws of rats was removed from the horizontal bar (mean ± SEM, N = 8–9 rats each). *P<0.05, **P<0.01, ***P<0.001, compared with vehicle-infused control rats; +P<0.05, ++P<0.01, +++P<0.001, compared with the value of session #1 by Fisher's LSD. Note: The pallidal infusion of the D2-like receptor agonist to control rats (green star) significantly reduced the latency.
doi:10.1371/journal.pone.0025831.g008

dopaminergic neurotransmission and dopamine-associated behavioral traits. The present analyses of this model provided us with the following information: 1) The hyperdopaminergic phenotype was maintained in the globus pallidus until adulthood. 2) The amounts of pallidal dopamine release were elevated at the adult stage of EGF-treated rats and normalized with antipsychotic treatment. 3) The reserpine-driven reduction in pallidal dopamine pool ameliorated the PPI deficits of EGF-treated rats. 4) The D2-like receptor blocker also normalized PPI levels of EGF-treated rats without affecting the catalepsy index. 5) Conversely, local administration of the D2-like receptor agonist to naïve rats caused deficits in PPI and bar-hang latency similar to that seen in EGF-treated rat. These results reveal that EGF exposure to rat pups produces persistent neurotrophic influences on the nigropallidal dopamine neurons and their functions. Thus, we postulate that the behavioral deficits of this EGF model, in part, can be ascribed to the D2 receptor-dependent hyperdopaminergic states of this basal ganglia circuit.

Trophic actions and selectivity of epidermal growth factor peripherally administered

EGF and other ErbB ligands (such as neuregulin-1) are neurotrophic not only for midbrain dopaminergic neurons but also for GABAergic neurons and glial cells [1–5], [37], [38]. Although we have been investigating the phenotypic influences of peripheral EGF challenges on developing GABAergic and glial cells, these effects did not persist until the adult stage [2], [26], [31]. As such, the hyperdopaminergic influence found in the present investigation is the sole phenotypic change that we have detected in the adult stage of EGF-treated rats. Similar to this study, we find long-lasting influences of neonatal neuregulin-1 challenges on the dopamine system [4]. With the given widespread action of these ErbB ligands, however, we cannot rule out the possibility that undetected changes in GABAergic or glial phenotype or function still remain in this model [2], [5], [37], [38].

Individual dopaminergic systems of mesostriatal, mesolimbic, and mesofrontocortical pathways appear to be differentially regulated by individual neurotrophic factors [5], [37–39]. Among these neurons, a subset of dopaminergic neurons in the ventral tier of the substantia nigra pars compacta mainly express the EGF receptor (ErbB1), which constitute of highly branched dopaminergic neurons in the mesostriatal and pallidal pathways [5], [40], while the neuregulin-1 receptors (ErbB4) are most enriched in mesofrontocortical dopamine neurons [37]. Therefore, it is likely that mesostriatal dopaminergic population responded to exogenous EGF and contributed to the pallidal hyperdopaminergic states of the present animal model. In contrast to the neurochemical changes, the number of dopamine terminals in the globus pallidus was less remarkable. In this context, the neurotrophic feature of EGF on dopamine neurons remains to be fully characterized; its effects on cell survival, phenotypic enhancement, or terminal arborization. Our preliminary study failed to detect apparent difference in the number of dopamine neurons (data not shown).

In contrast to the present EGF model, the mice treated with neuregulin-1 as neonates, in which dopaminergic influences are most pronounced in the prelimbic cortex, exhibit less marked deficits in PPI but more severe impairments in social behaviors [4], [41]. The difference of the behavioral traits between the two models might reflect the distinct neurotrophic actions of EGF and neuregulin-1 on these cell subpopulations.

Neuropathological implication of the globus pallidus for schizophrenia and its animal model

The globus pallidus is part of the indirect pathway of the basal ganglia circuit and receives dopaminergic innervation [42], [43]. The pathway initiates from the medium spiny neurons (MSN) in the striatum carry dopamine D2 receptors [44–46] and regulates sensorimotor gating, motor coordination, attention, learning and antipsychotic pharmacology [47–51]. Kodsi and Swerdlow (1995) showed that parts of globus pallidus, the ventral and caudal pallidum, are involved in sensorimotor gating [50]. The preceding report does not contradict the present finding although we did not distinguish these subregions of the globus pallidus. The dopaminergic abnormality in the indirect pathway represents one of the neuropathological features of this model and contributes to its behavioral deficits.

With respect to the antipsychotic effect of the D2 receptor antagonism in the indirect pathway, however, several controversies still remain; systemic administration of haloperidol failed to result in clear PPI improvement in EGF-treated rats [26]. In this context, neurobehavioral consequences of D2 receptor antagonism may significantly differ depending upon the brain regions where the antagonist acts [50]. Although we made the best efforts to minimize the technical artifacts and variations of cannula implantation, we cannot fully rule out aversive influences of the microsurgery on behavioral testing. The regional specificity of the drug actions should warrant future independent studies. As far as we compared the animals in control and experimental groups that equally received the surgery, however, the anti-dopaminergic manipulations produced the consistent results in behavioral tests.

The inhibition of dopamine D2 receptor at presynaptic sites of MSN fibers facilitates GABA release in the globus pallidus, leading to motor dysfunction such as catalepsy [42], [52–55]. In accordance with this cataleptic mechanism, our intrapallidal infusion of the D2-like receptor antagonist to control rats resulted in an increase in the catalepsy index while the D2-like receptor agonist conversely decreased the catalepsy index. We observed a similar D2-like receptor-dependency of the agonist and antagonist in the PPI paradigm. These results suggest the possibility that these behavioral deficits of EGF-treated rats involve the hyper-activation of D2-like receptors. However, the abnormalities of the present model in social behavior and pulse-alone startle appeared to be distinct from the pallidal dopamine neuropathology. In this context, EGF-treated rats should have the unrevealed structural or phenotypic alteration(s) underlying these behavioral impairments. Whether these impairments also involve the dopamine system remains to be investigated.

Of note, alterations in pallidal morphology and abnormal activation of this brain region are often implicated in schizophrenia. Brain imaging studies reveal pallidal structural abnormalities in schizophrenia patients [56–61]. Functional imaging also suggests an activation impairment in this brain region of patients [62], [63]. These abnormalities might have any association with the pallidal hyperdopaminergic states found in the present EGF model, especially if excess dopamine exerts neurotrophic and cell mitotic activities on pallidal cells and increases the tissue volume or function [64].

Vulnerability of midbrain dopaminergic development to neurotrophic cytokines

Schizophrenia animal models established by maternal immune challenges or neonatal hypoxia appear to support the dopamine hypothesis for schizophrenia although several controversies still remain [65–67]. For example, the animal model established by maternal challenge with bacterial lipopolysaccharide shows a long-lasting increase in TH levels and dopamine turnover, at least, in the nucleus accumbens [68], [69]. Perinatal asphyxia and viral infection also result in distinct abnormalities in the dopamine system [70–74]. Our preceding study suggests that neuregulin-1, another ErbB receptor ligand, also induce several behavioral abnormalities relevant to schizophrenia, when neuregulin-1 is administered to newborn mice [4]. These findings indicate the possibility that the phenotypic and functional abnormalities in these immune/inflammatory models might involve EGF or other ErbB ligand(s) acting on midbrain dopamine neurons at prenatal or perinatal stages [25].

In conclusion, the developmental regulation of midbrain dopaminergic neurons is more vulnerable against peripheral cytokine signals than previously thought. The present results indicate that perinatal and potentially prenatal exposure to EGF or EGF-related cytokines may produce crucial and persistent impact on dopaminergic innervation and function in the indirect pathway of the basal ganglia circuit. In light of dopamine D2 receptor antagonism, which is commonly implicated in antipsychotic pharmacology, the present cytokine model may help to elucidate its antipsychotic mechanism as well as to validate the dopamine hypothesis for schizophrenia.

Materials and Methods

Ethics statement

All of the animal experiments described were approved by the Animal Use and Care Committee guidelines of Niigata University (Approval No18 on April 26, 2010) and performed in accordance with the guidelines of NIH-USA. Every effort was made to minimize the discomfort of the animals in addition to the number of animals used in the experiments.

Animals

Male newborn Sprague-Dawley rats (SLC Ltd., Hamamatsu, Japan) were housed with a dam under a 12-h light/dark cycle (lights on 8:00 a.m.) in a plastic cage (276×445×205 mm). The rats were allowed free access to food and water. After weaning [postnatal day (PND) 20–30], rats were separated and housed with 2–3 rats per cage. Each adult animal (PND 56–94) was used in each experiment. Naïve Sprague-Dawley rats (all male, PND 56–70; SLC) were also used in control experiments. Recombinant human EGF (Higeta Shouyu Co., Chiba Japan) was dissolved in saline. EGF (0.875 μg/g) was administered subcutaneously (s.c.) each day to half of the littermates during PND 2–10 [26]. Control littermates received an injection of the same dose of cytochrome c (control protein) on the same schedule. The dose of EGF used in this study did not produce any apparent growth retardation in rats and mice [26], [28]. Some of adult rats daily received risperidone (1 mg/kg, i.p.; Janssen Pharmaceuticals Inc) or saline for 14 days.

Enzyme-linked immunosorbent assay (ELISA)

Rats were anesthetized with halothane, and brains were removed and cut into 1-mm thick slices. Using published boundaries [75], we identified and punched out each brain region of interest. TH levels were measured using ELISA [10]. In brief, brain tissues were homogenized in 10 volumes of homogenization buffer [0.1 mM phenylmethanesulfonyl fluoride, 0.1 mM benzethonium chloride, 1 mM benzamidine (Sigma Chemical Co., St. Louis, MO), and 10 μg/ml aprotinin]. Brain homogenates were centrifuged at 14000× g for 20 min at 4°C, and the supernatants were stored at −80°C until use. Protein concentrations were determined using a Micro BCA kit (Pierce, Rockland, IL) with bovine serum albumin (BSA) as a standard.

Tissue homogenates or striatal lysates (standards) were loaded into ELISA plate wells coated with mouse monoclonal anti-TH antibody (a gift from Dr. Hatanaka and Dr. Takei). Plates were incubated with rabbit polyclonal anti-TH antibody (Chemicon, Temecula, CA) followed by incubation with anti-rabbit IgG β-galactosidase (1:1000, American Qualex, San Clemente, CA). The fluorescence of the enzyme products from a reaction with 4-methylumbelliferyl-β-D-galactoside (MUG, Sigma) was measured using a microplate reader (COLONA electric Co., Ltd., Ibaraki, Japan).

Immunoblotting

Each brain tissue was dissected as described above and homogenized in 200 μl lysis buffer [2% sodium dodecylsulfate (SDS), 10 mM Tris-HCl buffer (pH 7.4), 5 mM ethylenediamine-

N,N,N',N'-tetraacetic acid (EDTA), 10 mM NaF, 2 mM Na_3VO_4, 0.5 mM phenylarsine oxide], and boiled at 95°C for 5 min. After centrifugation at 12000 rpm for 20 min, the supernatant was harvested. The supernatant was mixed with 5× sample buffer [0.31 M Tris-HCl (pH 6.8), 10% SDS, 50% glycerol, 25% 2-mercaptoethanol] and boiled at 95°C for 5 min. Denatured protein samples were subjected to 7.5% SDS-polyacrylamide gel electrophoresis and transferred to a nitrocellulose membrane (Schleicher and Schull, Dassel, Germany) by electrophoresis. The membrane was probed with anti-TH (1:2000, Chemicon), anti-vesicular monoamine transporter 2 (VMAT2) (1:1000, Chemicon), anti-dopamine-beta-hydroxylase (DβH) (1:500, Chemicon), anti-dopamine D1 receptor (1:1000, Sigma) or anti-D2 receptor (1:1000, Chemicon) antibodies. After washing, membrane immunoreactivity was detected using anti-rat, anti-rabbit, or anti-mouse immunoglobulin antibody conjugated to horseradish peroxidase (Jackson Immunoresearch Laboratory, West Grove, PA) followed by a chemiluminescence reaction (ECL kit, GE Health Science Inc., Tokyo, Japan) and exposure to X-ray films. Film images carrying a liner range of darkness of bands were subjected to film scanning and converted to the 8-bit digital data. Densitometric quantification of band intensity was performed with the free software Image J (National Institutes of Health, USA).

Immunohistochemistry

Rats were anesthetized with halothane, perfused transcardially for 7 min with phosphate-buffered saline (150 mM NaCl, 0.1 M sodium phosphate; pH 7.5) followed by 4% paraformaldehyde in phosphate-buffered saline. Brains were removed and post-fixed in the same fixation solution for 24 h at 4°C. Fixed brains were immersed in 30% sucrose solution for 3–5 days, and frozen in resin (Tissue-Tek, Sakura Finetek U.S.A. Inc. Torrance, CA). Sections (40 μm) were cut with a cryostat (CM1510, Leica, Nussloch, Germany). After rinsing in Tris-buffered saline [TBS; 0.1 M Tris-HCl (pH 7.4), 150 mM NaCl] containing 0.2% Triton X-100, sections were pretreated with 6% BSA and 0.2% Triton X-100 in TBS and then incubated with anti-TH antibody (1:1000, Chemicon) in TBS containing 3% BSA and 0.2% Triton X-100 for 48–72 h at 4°C. After rinsing in TBS/0.2% Triton X-100 three times, sections were incubated with biotinylated anti-rabbit immunoglobulin antibody (1:200, Jackson Immunoresearch Laboratory). Immunoreactivity was visualized using a Vectastain Elite ABC kit (Vector Laboratories, Burlingame, CA) using diaminobenzidine as a substrate.

Determination of monoamine contents

Each brain region was homogenized in 0.1 M perchloric acid containing 0.1 mM EDTA, and 100 nM isoproterenol. After centrifugation at 12000 rpm for 20 min, the supernatants and pellets were harvested. Concentrations of dopamine and its metabolites, 3,4-dihydroxyphenylacetic acid (DOPAC) and homovanillic acid (HVA), in supernatants were analyzed by HPLC-electrochemistry [4]. The mobile phase containing 50 mM trisodium citrate (pH 3.2), 25 mM NaH_2PO_4, 10 mM diethylamine, 0.03 mM EDTA, 2.5 mM 1-octane sulfonic acid sodium salt, 6% methanol, 1% dimethylacetamide was delivered at 0.5 mL/min. Monoamines were separated on an analytical HPLC column (CA-50DS, 4.6×150 mm, Eicom, Kyoto, Japan) and detected with a graphite electrode (WE-3G, Eicom) to which +700 mV was applied. Data analysis was performed with a data acquisition computer (Powerchrom, Eicom). Tissue pellets were homogenized in 0.5 N NaOH and subjected to protein determination with a Micro BCA kit (see above). Tissue monoamine contents were normalized with protein concentrations.

Local drug administration to the globus pallidus

Control and EGF-treated rats (PND 56–70) were anesthetized with sodium pentobarbital (65 mg/kg, i.p.). After confirming deep anesthesia, a rat was mounted on a stereotaxic apparatus with an incisor bar set at 3.3 mm below the interaural line. The skull was exposed and two holes were drilled for bilateral implantation of guide cannulae (23 G stainless-steel pipes) into the GP. The stereotaxic coordinates were 0.9 mm anterior, ±3.0 mm lateral from the bregma, and 4.5 mm below the dura mater. After allowing the rat at least 10 days of recovery from surgery, a 30-G needle connected to Teflon tubing and a Hamilton syringe was placed 2 mm below the tip of the guide cannula. The drug (0.5 μl) was injected over a period of 30 sec, and the needle left in place for an additional 30 sec. Rats were placed in their home cage for 5–15 min, to allow for local diffusion of the drug; the rats were then subjected to behavioral tests (see below). When rats received reserpine, rats were placed in their home cage for 120 min to deplete the local dopamine pool. The cannula position was confirmed after the completion of the behavioral tests (see below).

Reserpine (Daiichi Sankyo Pharmaceutical Inc., Tokyo, Japan) was dissolved in phosphate-buffered solution (pH 4.0) containing 3 mg/mL DL-methionine and 70 mg/mL propylene glycol. Conventional dopamine receptor ligands, SCH23390, raclopride and quinpirole, were all obtained from Sigma and dissolved in 10% dimethyl sulfoxide (DMSO) in saline (vehicle).

Microdialysis

Rats were anesthetized with sodium pentobarbital (65 mg/kg i.p.) and mounted in a stereotaxic apparatus. The skull was exposed and a hole was drilled for unilateral implantation of a guide cannula (AG-8, Eicom) into the GP. The stereotaxic coordinates were 0.9 mm anterior; 3.0 mm lateral from the bregma, and 4.8 mm below the dura mater. After allowing the rat at least 10 days of recovery from surgery microdialysis experiments were performed.

The microdialysis probe (2 mm active area, A-I-8-02, Eicom) was connected to Teflon tubing (0.65 mm o.d., 0.12 mm i.d.; Bioanalytical Systems Inc., West Lafayette, IN). The rat was perfused with artificial cerebrospinal fluid (pH 7.0) containing 147 mM NaCl, 2.7 mM KCl, 1.2 mM $CaCl_2$, and 0.5 mM $MgCl_2$ at a flow rate of 0.7 μL/min. Dialysate was discarded to obtain a steady state for at least 18 h after implantation of the probe, and then dialysate samples were collected every 30 min. The first five fractions were collected to determine basal levels of dopamine. The perfusion medium was switched to the medium containing a high concentration of potassium (80 mM KCl, 69.7 mM NaCl, 1.2 mM $CaCl_2$, 0.5 mM $MgCl_2$; pH 7) for 60 min (for two fractions). The perfusion medium was then switched back to the original medium and five fractions were additionally collected. In all, total 12 fractions were collected.

Dopamine in the dialysates was determined by HPLC with electrochemical detection. The mobile phase containing 48 mM citric acid, 24 mM sodium acetate, 10 mM NaCl, 0.5 mM EDTA, 2.5 mM SDS, and 16% acetonitrile (pH 4.8) was delivered at 50 μL/min. Dopamine was separated on an analytical column (BDS Hypersil C18 1×100 mm, Thermo Fisher Scientific, Yokohama, Japan) and detected with a 3 mm glassy carbon electrode detector (Unijet flow cell; Bioanalytical Systems Inc.) to which +550 mV was applied. Data analysis was performed with the analysis software (Epsilon LC; Bioanalytical Systems Inc.). Data were not compensated with the recovery rate.

Confirmation of cannula positioning

After local drug injection or microdialysis, rats were deeply anesthetized with halothane and decapitated. Brains were quickly removed and fixed in 4% paraformaldehyde for 3 days. Fixed brains were cut into 50-μm sections using a vibratome (Dosaka EM Ltd., Kyoto, Japan). Each section was stained with 0.5% cresyl violet solution. The location of a microdialysis probe or injection needle was determined under a microscope according to a stereotaxic atlas [75]. Animals that exhibited incorrect cannula placement were removed from the data analysis.

Measurement of acoustic startle and prepulse inhibition of startle response

Acoustic startle amplitude was measured in a startle chamber (SR-Lab Systems, San Diego Instruments, San Diego, CA) [34]. Rats were placed into a startle chamber with 70-dB background noise. Five minutes later, the startle amplitude was recorded in a session that included multiple trial types: (i) a 120-dB 40-ms noise burst presented alone (pulse); (ii–iv) 40-ms 120-dB noise burst following prepulses by 100 ms (20-ms noise burst) that were 5, 10, and 15 dB above background noise (i.e., 75-, 80-, 85-dB prepulse, respectively); and (v) no stimulus (background noise alone). The percentage PPI of startle responses was calculated as: $100-[(\text{startle response on prepulse-pulse stimulus trials} - \text{no stimulus trials})/(\text{pulse-alone trials} - \text{no stimulus trials})]\times 100$. To match the magnitude of pulse alone startles between groups, a 120-dB noise burst was replaced with a 110-dB noise burst in some experiments.

Analysis of locomotor activity

Side effects of reserpine were estimated by monitoring spontaneous locomotor activity under novel conditions. Reserpine-infused rats were placed in an open field box (45 cm length×45 cm width×30 cm height, MED Associates, St. Albans, VA, USA) under a moderate light level (200 Lx). Line crossings and rearing counts were measured by photo-beam sensors (25 mm intervals for horizontal axis and 150 mm for vertical axis).

Social interaction test

The index for social interaction of rats was measured according to Futamura et al. (2003) [26]. Following the above locomotor test, reserpine- or vehicle-infused rats were exposed to an unfamiliar male rat that was housed in another cage, and was age, body-weight, and gender-matched. All tests were videotaped and scored in blind. Scoring of social interaction times and duration was based on sniffing behaviors, defined as active chasing of the partner, shaking the nose near the partner, and contacting the partner with the nose.

Measurement of immobilization levels in the bar-hang test

Immobilization levels and the cataleptic effects of drugs were measured using a bar-hang test method [76]. In the bar-hang test, the front paws of the rat were gently placed on a horizontal metal bar (5 mm diameter) and placed 10 cm above ground level. The test was terminated when the paw of animal was released from the bar or 300 sec had passed, and the total time until the animals removed the paw from the bar was recorded. Rats were subjected to three blocks (separated by 20-min intervals) of three trials. Scores at the three different time blocks (after 1-h acclimation, 20 and 40 min after drug infusion) were monitored for comparison purposes.

Statistical analysis

All data are expressed as means ± SEM. Statistical differences in the behavioral data were determined by analysis of variance (ANOVA). When univariate data were obtained from two groups, two-tailed *t*-test was used for comparison. Behavioral scores were initially subjected to factorial ANOVA using neonatal EGF treatment (two levels) and local drug infusion (two or three levels) as between-subjects factors, and prepulse magnitude (three levels) or test session (two levels) as a within-subjects factor. As the initial analyses yielded a significant factorial interaction, data were subjected to a Fisher's LSD *post-hoc* test with or without repeated measure. The interaction of a within-subjects factor with a between-subjects factor was estimated by multivariate analysis of variance (MANOVA). Individual statistical differences between data points are shown in the figures. Correlations between dopamine release and PPI were examined by Pearson's correlation analysis. A p value less than 0.05 was regarded as statistically significant. Statistical analyses were performed using StatView software (SAS Institute Inc., Cary, NC, USA). N values in parentheses represent the number of animals used in each group.

Acknowledgments

We thank Dr. Hatanaka and Dr. Takei for their gift of the monoclonal antibody for TH.

Author Contributions

Conceived and designed the experiments: H. Nawa. Performed the experiments: HS YZ YI MM MA KS RW. Analyzed the data: HS H. Nawa. Contributed reagents/materials/analysis tools: H. Namba. Wrote the paper: H. Nawa.

References

1. Woo RS, Li XM, Tao Y, Carpenter-Hyland E, Huang YZ, et al. (2007) Neuregulin-1 enhances depolarization-induced GABA release. Neuron 54: 599–610.
2. Nagano T, Namba H, Abe Y, Aoki H, Takei N, et al. (2007) In vivo administration of epidermal growth factor and its homologue attenuates developmental maturation of functional excitatory synapses in cortical GABAergic neurons. Eur J Neurosci 25: 380–390.
3. Fazzari P, Paternain AV, Valiente M, Pla R, Luján R, et al. (2010) Control of cortical GABA circuitry development by Nrg1 and ErbB4 signaling. Nature 464: 1376–1380.
4. Kato T, Abe Y, Sotoyama H, Kakita A, Kominami R, et al. (2011) Transient exposure of neonatal mice to neuregulin-1 results in hyperdopaminergic states in adulthood: implication in neurodevelopmental hypothesis for schizophrenia. Mol Psychiatry 16: 307–320.
5. Iwakura Y, Zheng YJ, Sibilia M, Abe Y, Piao YS, et al. (2011) Qualitative and quantitative re-evaluation of epidermal growth factor-ErbB1 action on developing midbrain dopaminergic neurons in vivo and in vitro: target-derived neurotrophic signaling (Part 1). J Neurochem 118: 45–56.
6. Stefansson H, Sigurdsson E, Steinthorsdottir V, Bjornsdottir S, Sigmundsson T, et al. (2001) Neuregulin 1 and susceptibility to schizophrenia. Am J Hum Genet 71: 877–892.
7. Munafò MR, Thiselton DL, Clark TG, Flint J (2006) Association of the NRG1 gene and schizophrenia: a meta-analysis. Mol Psychiatry 11: 539–546.
8. Anttila S, Illi A, Kampman O, Mattila KM, Lehtimäki T, et al. (2004) Association of EGF polymorphism with schizophrenia in Finnish men. Neuroreport 15: 1215–1218.
9. Benzel I, Bansal A, Browning BL, Galwey NW, Maycox PR, et al. (2007) Interactions among genes in the ErbB-Neuregulin signalling network are associated with increased susceptibility to schizophrenia. Behav Brain Funct 3: 31.
10. Futamura T, Toyooka K, Iritani S, Niizato K, Nakamura R, et al. (2002) Abnormal expression of epidermal growth factor and its receptor in the forebrain and serum of schizophrenic patients. Mol Psychiatry 7: 673–682.
11. Shibuya M, Komi E, Wang R, Kato T, Watanabe Y, et al. (2010) Measurement and comparison of serum neuregulin 1 immunoreactivity in control subjects and patients with schizophrenia: an influence of its genetic polymorphism. J Neural Transm 117: 887–895.

12. Chong VZ, Thompson M, Beltaifa S, Webster MJ, Law AJ, et al. (2008) Elevated neuregulin-1 and ErbB4 protein in the prefrontal cortex of schizophrenic patients. Schizophr Res 100: 270–280.
13. Hashimoto R, Straub RE, Weickert CS, Hyde TM, Kleinman JE, et al. (2004) Expression analysis of neuregulin-1 in the dorsolateral prefrontal cortex in schizophrenia. Mol Psychiatry 9: 299–307.
14. Zscheppang K, Korenbaum E, Bueter W, Ramadurai SM, Nielsen HC, et al. (2006) ErbB receptor dimerization, localization, and co-localization in mouse lung type II epithelial cells. Pediatr Pulmonol 41: 1205–1212.
15. Yarden Y, Sliwkowski MX (2001) Untangling the ErbB signaling network. Nat Rev Mol Cell Biol 2: 127–137.
16. Mei L, Xiong WC (2008) Neuregulin 1 in neural development, synaptic plasticity and schizophrenia. Nat Rev Neurosci 9: 437–452.
17. Harrison PJ, Law AJ (2006) Neuregulin 1 and schizophrenia: genetics, gene expression, and neurobiology. Biol Psychiatry 60: 132–140.
18. Patterson PH (2007) Maternal effects on schizophrenia risk. Science 318: 576–577.
19. Boksa P (2010) Effects of prenatal infection on brain development and behavior: a review of findings from animal models. Brain Behav Immun 24: 881–897.
20. Meyer U, Feldon J, Fatemi SH (2009) In-vivo rodent models for the experimental investigation of prenatal immune activation effects in neurodevelopmental brain disorders. Neurosci Biobehav Rev 33: 1061–1079.
21. Ehninger D, Sano Y, de Vries PJ, Dies K, Franz D, et al. (2010) Gestational immune activation and Tsc2 haploinsufficiency cooperate to disrupt fetal survival and may perturb social behavior in adult mice. Mol Psychiatry (doi: 10.1038/mp.2010.115) in press.
22. Varner MW, Dildy GA, Hunter C, Dudley DJ, Clark SL, et al. (1996) Amniotic fluid epidermal growth factor levels in normal and abnormal pregnancies. J Soc Gynecol Investig 3: 17–19.
23. Hofmann GE, Abramowicz JS (1990) Epidermal growth factor (EGF) concentrations in amniotic fluid and maternal urine during pregnancy. Acta Obstet Gynecol Scand 69: 217–221.
24. Virgintino D, Maiorano E, Errede M, Vimercati A, Greco P, et al. (1998) Astroglia-microvessel relationship in the developing human telencephalon. Int J Dev Biol 42: 1165–1168.
25. Nawa H, Takei N (2006) Recent progress in animal modeling of immune inflammatory processes in schizophrenia: implication of specific cytokines. Neurosci Res 56: 2–13.
26. Futamura T, Kakita A, Tohmi M, Sotoyama H, Takahashi H, et al. (2003) Neonatal perturbation of neurotrophic signaling results in abnormal sensorimotor gating and social interaction in adults: implication for epidermal growth factor in cognitive development. Mol Psychiatry 8: 19–29.
27. Mizuno M, Malta RS, Jr., Nagano T, Nawa H (2004) Conditioned place preference and locomotor sensitization after repeated administration of cocaine or methamphetamine in rats treated with epidermal growth factor during the neonatal period. Ann N Y Acad Sci 1025: 612–618.
28. Tohmi M, Tsuda N, Mizuno M, Takei N, Frankland PW, et al. (2005) Distinct influences of neonatal epidermal growth factor challenge on adult neurobehavioral traits in four mouse strains. Behav Genet 35: 615–629.
29. Iwakura Y, Wang R, Abe Y, Piao YS, Shishido Y, et al. (2011) Dopamine-dependent ectodomain shedding and release of epidermal growth factor in developing striatum: target-derived neurotrophic signaling (Part 2). J Neurochem. in press.
30. Tsuda N, Mizuno M, Yamanaka T, Komurasaki T, Yoshimoto M, et al. (2008) Common behavioral influences of the ErbB1 ligands transforming growth factor alpha and epiregulin administered to mouse neonates. Brain Dev 30: 533–543.
31. Namba H, Nagano T, Iwakura Y, Xiong H, Jourdi H, et al. (2006) Transforming growth factor alpha attenuates the functional expression of AMPA receptors in cortical GABAergic neurons. Mol Cell Neurosci 31: 628–641.
32. Prensa L, Giménez-Amaya JM, Parent A, Bernácer J, Cebrián C (2009) The nigrostriatal pathway: axonal collateralization and compartmental specificity. J Neural Transm Suppl 73: 49–58.
33. Rommelfanger KS, Wichmann T (2010) Extrastriatal dopaminergic circuits of the Basal Ganglia. Front Neuroanat 4: 139.
34. Swerdlow NR, Geyer MA, Braff DL (2001) Neural circuit regulation of prepulse inhibition of startle in the rat: current knowledge and future challenges. Psychopharmacology (Berl) 156: 194–215.
35. Brody SA, Dulawa SC, Conquet F, Geyer MA (2004) Assessment of a prepulse inhibition deficit in a mutant mouse lacking mGlu5 receptors. Mol Psychiatry 9: 35–41.
36. Ogren SO, Fuxe K (1988) D1- and D2-receptor antagonists induce catalepsy via different efferent striatal pathways. Neurosci Lett 85: 333–338.
37. Abe Y, Namba H, Zheng Y, Nawa H (2009) In situ hybridization reveals developmental regulation of ErbB1-4 mRNA expression in mouse midbrain: implication of ErbB receptors for dopaminergic neurons. Neuroscience 161: 95–110.
38. von Bohlen und Halbach O, Unsicker K (2009) Neurotrophic support of midbrain dopaminergic neurons. In: Development and Engineering of Dopamine Neurons. New York: Springer Science. pp 73–77.
39. Solbrig M, Fallon J, Liplin I (2004) Drawings of some other features of the SN-VTA, including dopamine transporter sites, cannabinoid receptors, and different nuclei and fiber tracts in the SN-VTA. In: Paxinos G, ed. The Rat Nervous System Australia: Academic Press. 229 p.
40. Kornblum HI, Gall CM, Seroogy KB, Lauterborn JC (1995) A subpopulation of striatal gabaergic neurons expresses the epidermal growth factor receptor. Neuroscience 69: 1025–1029.
41. Kato T, Kasai A, Mizuno M, Fengyi L, Shintani N, et al. (2011) Phenotypic characterization of transgenic mice overexpressing neuregulin-1. PLoS One 5: e14185.
42. Querejeta E, Delgado A, Valdiosera R, Erlij D, Aceves J (2001) Intrapallidal D2 dopamine receptors control globus pallidus neuron activity in the rat. Neurosci Lett 300: 79–82.
43. Fuchs H, Hauber W (2004) Dopaminergic innervation of the rat globus pallidus characterized by microdialysis and immunohistochemistry. Exp Brain Res 154: 66–75.
44. Gerfen CR, Engber TM, Mahan LC, Susel Z, Chase TN, et al. (1990) D1 and D2 dopamine receptor-regulated gene expression of striatonigral and striatopallidal neurons. Science 250: 1429–1432.
45. Smith Y, Bevan MD, Shink E, Bolam JP (1998) Microcircuitry of the direct and indirect pathways of the basal ganglia. Neuroscience 86: 353–387.
46. Sano H, Yasoshima Y, Matsushita N, Kaneko T, Kohno K, et al. (2003) Conditional ablation of striatal neuronal types containing dopamine D2 receptor disturbs coordination of basal ganglia function. J Neurosci 23: 9078–9088.
47. Takahashi K, Nagai T, Kamei H, Maeda K, Matsuya T, et al. (2007) Neural circuits containing pallidotegmental GABAergic neurons are involved in the prepulse inhibition of the startle reflex in mice. Biol Psychiatry 62: 148–157.
48. Qu Y, Swerdlow NR, Weber M, Stouffer D, Parsons LH (2008) Quinelorane, a dopamine D3/D2 receptor agonist, reduces prepulse inhibition of startle and ventral pallidal GABA efflux: time course studies. Pharmacol Biochem Behav 90: 686–690.
49. Qu Y, Saint Marie RL, Breier MR, Ko D, Stouffer D, et al. (2009) Neural basis for a heritable phenotype: differences in the effects of apomorphine on startle gating and ventral pallidal GABA efflux in male Sprague-Dawley and Long-Evans rats. Psychopharmacology (Berl) 207: 271–280.
50. Kodsi MH, Swerdlow NR (1995) Prepulse inhibition in the rat is regulated by ventral and caudodorsal striato-pallidal circuitry. Behav Neurosci 109: 912–928.
51. Sotoyama H, Namba H, Takei N, Nawa H (2007) Neonatal exposure to epidermal growth factor induces dopamine D2-like receptor supersensitivity in adult sensorimotor gating. Psychopharmacology (Berl) 191: 783–792.
52. Hauber W, Lutz S (1999) Dopamine D1 or D2 receptor blockade in the globus pallidus produces akinesia in the rat. Behav Brain Res 106: 143–150.
53. Fuchs H, Hauber W (2004) Changes in extracellular dopamine in the rat globus pallidus induced by typical and atypical antipsychotic drugs. Neurochem Int 45: 1029–1038.
54. Chiken S, Shashidharan P, Nambu A (2008) Cortically evoked long-lasting inhibition of pallidal neurons in a transgenic mouse model of dystonia. J Neurosci 28: 13967–13977.
55. Bouali-Benazzouz R, Tai CH, Chetrit J, Benazzouz A (2009) Intrapallidal injection of 6-hydroxydopamine induced changes in dopamine innervation and neuronal activity of globus pallidus. Neuroscience 164: 588–596.
56. Hokama H, Shenton ME, Nestor PG, Kikinis R, Levitt JJ, et al. (1995) Caudate, putamen, and globus pallidus volume in schizophrenia: a quantitative MRI study. Psychiatry Res 61: 209–229.
57. Gur RE, Maany V, Mozley PD, Swanson C, Bilker W, et al. (1998) Subcortical MRI volumes in neuroleptic-naive and treated patients with schizophrenia. Am J Psychiatry 155: 1711–1717.
58. Spinks R, Nopoulos P, Ward J, Fuller R, Magnotta VA, et al. (2005) Globus pallidus volume is related to symptom severity in neuroleptic naive patients with schizophrenia. Schizophr Res 73: 229–233.
59. Mamah D, Wang L, Barch D, de Erausquin GA, Gado M, et al. (2007) Structural analysis of the basal ganglia in schizophrenia. Schizophr Res 89: 59–71.
60. Goldman AL, Pezawas L, Mattay VS, Fischl B, Verchinski BA, et al. (2008) Heritability of brain morphology related to schizophrenia: a large-scale automated magnetic resonance imaging segmentation study. Biol Psychiatry 63: 475–483.
61. Hashimoto R, Mori T, Nemoto K, Moriguchi Y, Noguchi H, et al. (2009) Abnormal microstructures of the basal ganglia in schizophrenia revealed by diffusion tensor imaging. World J Biol Psychiatry 10: 65–69.
62. Early TS, Reiman EM, Raichle ME, Spitznagel EL (1987) Left globus pallidus abnormality in never-medicated patients with schizophrenia. Proc Natl Acad Sci USA 84: 561–563.
63. Menon V, Anagnoson RT, Glover GH, Pfefferbaum A (2001) Functional magnetic resonance imaging evidence for disrupted basal ganglia function in schizophrenia. Am J Psychiatry 158: 646–649.
64. Iwakura Y, Nawa H, Sora I, Chao MV (2008) Dopamine D1 receptor-induced signaling through TrkB receptors in striatal neurons. J Biol Chem 283: 15799–15806.
65. Goto Y, Grace AA (2007) The dopamine system and the pathophysiology of schizophrenia: a basic science perspective. Int Rev Neurobiol 78: 41–68.
66. Toda M, Abi-Dargham A (2007) Dopamine hypothesis of schizophrenia: making sense of it all. Curr Psychiatry Rep 9: 329–336.
67. Simpson EH, Kellendonk C, Kandel E (2010) A possible role for the striatum in the pathogenesis of the cognitive symptoms of schizophrenia. Neuron 65: 585–596.
68. Borrell J, Vela JM, Arévalo-Martin A, Molina-Holgado E, Guaza C (2002) Prenata immune challenge disrupts sensorimotor gating in adult rats.

Implications for the etiopathogenesis of schizophrenia. Neuropsychopharmacology 26: 204–215.
69. Romero E, Guaza C, Castellano B, Borrell J (2010) Ontogeny of sensorimotor gating and immune impairment induced by prenatal immune challenge in rats: implications for the etiopathology of schizophrenia. Mol Psychiatry 15: 372–383.
70. El-Khodor BF, Boksa P (1997) Long-term reciprocal changes in dopamine levels in prefrontal cortex versus nucleus accumbens in rats born by Caesarean section compared to vaginal birth. Exp Neurol 145: 118–129.
71. Wakuda T, Matsuzaki H, Suzuki K, Iwata Y, Shinmura C, et al. (2008) Perinatal asphyxia reduces dentate granule cells and exacerbates methamphetamine-induced hyperlocomotion in adulthood. PLoS One 3: e3648.
72. Winter C, Djodari-Irani A, Sohr R, Morgenstern R, Feldon J, et al. (2009) Prenatal immune activation leads to multiple changes in basal neurotransmitter levels in the adult brain: implications for brain disorders of neurodevelopmental origin such as schizophrenia. Int J Neuropsychopharmacol 12: 513–524.
73. Winter C, Reutiman TJ, Folsom TD, Sohr R, Wolf RJ, et al. (2008) Dopamine and serotonin levels following prenatal viral infection in mouse–implications for psychiatric disorders such as schizophrenia and autism. Eur Neuropsychopharmacol 18: 712–716.
74. Vuillermot S, Weber L, Feldon J, Meyer U (2010) A longitudinal examination of the neurodevelopmental impact of prenatal immune activation in mice reveals primary defects in dopaminergic development relevant to schizophrenia. J Neurosci 30: 1270–1287.
75. Paxinos G, Watson C (1986) The Rat Brain in Stereotaxic Coordinates. San Diego: Academic Press.
76. Marchese G, Casti P, Ruiu S, Saba P, Sanna A, et al. (2003) Haloperidol, but not clozapine, produces dramatic catalepsy in delta9-THC-treated rats: possible clinical implications. Br J Pharmacol 140: 520–526.